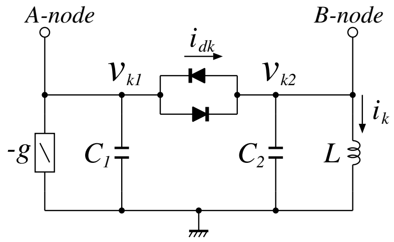

Fig. 3. Subcircuit 1.

$$x_k = \frac{v_{k1}}{V_{th}}, \quad y_k = \frac{v_{k2}}{V_{th}}, \quad z_k = \frac{1}{V_{th}}\sqrt{\frac{L}{C_2}}i_k,$$
$$t = \sqrt{LC_2}\tau, \quad \text{“}\cdot\text{”} = \frac{d}{d\tau}, \quad \alpha = \frac{C_2}{C_1}, \tag{1}$$
$$\beta = g\sqrt{\frac{L}{C_2}}, \quad \gamma = G_d\sqrt{\frac{L}{C_2}}, \quad \delta = \frac{1}{R}\sqrt{\frac{L}{C_2}},$$

Normalized circuit equations are described as follows: Subcircuit A ($1 \le k \le m$):

$$\begin{cases} \dot{x}_k = & \alpha\beta x_k - \alpha\gamma f(x_k - y_k) \\ & +\alpha\delta\{\sum_{i=n+1}^{m+n} x_i + \sum_{j=1}^{n} y_j - (m+n)x_k\}, \\ \dot{y}_k = & \gamma f(x_k - y_k) - z_k, \\ \dot{z}_k = & (1+p_k)y_k. \end{cases} \tag{2}$$

Subcircuit B ($m+1 \le k \le m+n$):

$$\begin{cases} \dot{x}_k &=& \alpha\beta x_k - \alpha\gamma f(x_k - y_k), \\ \dot{y}_k &=& \delta\{\sum_{i=n+1}^{m+n} x_i + \sum_{j=1}^{n} y_j \\ && -(m+n)y_k\} + \gamma f(x_k - y_k) - z_k, \\ \dot{z}_k &=& (1+q_k)y_k, \end{cases} \tag{3}$$

The nonlinear function $f(x)$ corresponding to the characteristics of the diodes is described as follows:

$$f(x) = x + \frac{(|x-1| - |x+1|)}{2}.$$

B. System 2

The subcircuit of System 2 is same as the subcircuit of System 1. However, only A-node is used in this system. An asymmetry of the system is realized as a difference of parameters. Namely, parameters of subcircuit A in Fig. 1 is different from subcircuit B. Using the following parameters

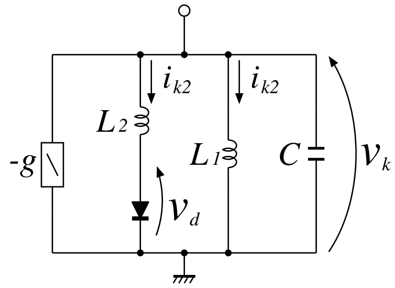

Fig. 4. Subcircuit 2.

and variables,

$$x_k = \frac{v_{k1}}{V_{th}}, \quad y_k = \frac{v_{k2}}{V_{th}}, \quad z_k = \frac{1}{V_{th}}\sqrt{\frac{L_a}{C_{2a}}},$$
$$t = \sqrt{L_a C_{2a}}\tau, \quad \text{“}\cdot\text{”} = \frac{d}{d\tau}, \quad \alpha = \frac{C_{2a}}{C_{1a}},$$
$$\beta = g\sqrt{\frac{L_a}{C_{2a}}}, \quad \gamma = G_d\sqrt{\frac{L_a}{C_{2a}}}, \quad \delta = G\sqrt{\frac{L_a}{C_{2a}}}, \tag{4}$$
$$\varepsilon = \frac{C_{2a}}{C_{1b}}, \quad \zeta = \frac{C_{2a}}{C_{2b}} \quad \text{and} \quad \eta = \frac{L_a}{L_b}.$$

Normalized circuit equations are described as follows: Subcircuit A ($1 \le k \le m$):

$$\begin{cases} \dot{x}_k = & \alpha\beta x_k - \alpha\gamma f(x_k - y_k) \\ & +\alpha\delta\left\{\sum_{i=1}^{m+n} x_i - (m+n)x_k\right\}, \\ \dot{y}_k = & -z_k + \gamma f(x_k - y_k), \\ \dot{z}_k = & (1+p_k)y_k, \end{cases} \tag{5}$$

Subcircuit B ($m+1 \le k \le m+n$):

$$\begin{cases} \dot{x}_k = & \varepsilon\beta x_k - \varepsilon\gamma f(x_k - y_k) \\ & +\varepsilon\delta\left\{\sum_{i=1}^{m+n} x_i - (m+n)x_k\right\}, \\ \dot{y}_k = & \zeta\left\{-z_k + \gamma f(x_k - y_k)\right\}, \\ \dot{z}_k = & \eta(1+q_k)y_k, \end{cases} \tag{6}$$

where,

$$f(x) = x + \frac{(|x-1| - |x+1|)}{2}.$$

C. System 3

The subcircuit of System 3 is shown in Fig. 4. This chaotic circuit was proposed by Inaba et al.[7]. Using the following parameters and variables,

$$\begin{aligned}
&x_k = \sqrt{\frac{L_{1a}}{C_a}}\frac{i_{k1}}{V_{th}}, \quad y_k = \sqrt{\frac{L_{1a}}{C_a}}\frac{i_{k2}}{V_{th}}, \quad z_k = \frac{v_k}{V_{th}},\\
&t = \sqrt{L_{1a}C_a}\tau, \quad \text{“}\cdot\text{”} = \frac{d}{d\tau}, \quad \alpha = \frac{L_{1a}}{L_{2a}},\\
&\beta = g_a\sqrt{\frac{L_{1a}}{C_a}}, \quad \gamma = r_d\sqrt{\frac{C_a}{L_{1a}}}, \quad \delta = G\sqrt{\frac{L_{1a}}{C_a}}, \qquad (7)\\
&\varepsilon = \frac{L_{1a}}{L_{1b}}, \quad \zeta = \frac{L_{1a}}{L_{2b}}, \quad \eta = \frac{C_a}{C_b},\\
&\text{and} \quad \theta = \frac{g_b}{g_a}.
\end{aligned}$$

Normalized circuit equations are described as follows:
Subcircuit A ($1 \le k \le m$):

$$\begin{cases}
\dot{x}_k = & (1+p_k)z_k\\
\dot{y}_k = & \alpha\left\{z_k - f(y_k)\right\},\\
\dot{z}_k = & -x_k - y_k + \beta z_k\\
& +\delta\{\sum_{i=1}^{m+n} z_i - (m+n)z_k,\}
\end{cases} \qquad (8)$$

Subcircuit B ($m+1 \le k \le m+n$):

$$\begin{cases}
\dot{x}_k = & (1+q_k)z_k\\
\dot{y}_k = & \zeta\left\{z_k - f(y_k)\right\},\\
\dot{z}_k = & \eta[-x_k - y_k + \beta\theta z_k\\
& +\delta\{\sum_{i=1}^{m+n} z_i - (m+n)z_k,\}]
\end{cases} \qquad (9)$$

where,

$$f(y_k) = \frac{\gamma y_k + 1 - |\gamma y_k - 1|}{2}.$$

III. COMPUTER SIMULATION

At first, each results of the computer simulations are shown. Figures 5 are examples of the computer simulation results on System 2. Double scroll type attractors are observed on the each subcircuits. In the case of System 1, similar attractors can be observed. Figures 6 are examples of the computer simulation results on System 3. Rossler type attractors are observed. Figure 7 shows the voltage differences between each

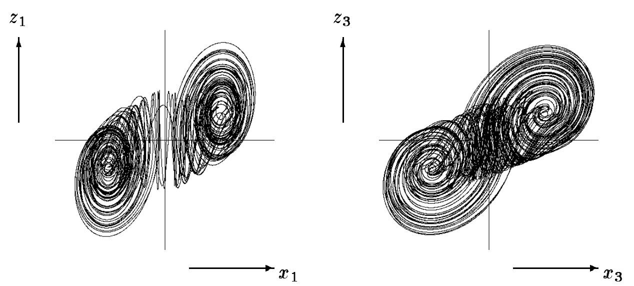

(a) Subcircuit A ($k = 1$) (b) Subcircuit B ($k = 3$)

Fig. 5. Attractors of System 1. Horizontal axes are x_k and vertical axes are z_k.

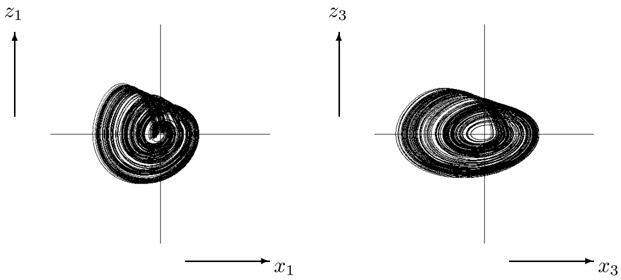

(a) Subcircuit A ($k = 1$) (b) Subcircuit B ($k = 3$)

Fig. 6. Attractors of System 1. Horizontal axes are x_k and vertical axes are z_k.

subcircuits in the case of System 2. Vertical axes show voltage differences and horizontal axes show time. Namely, in the case of synchronizing two subcircuits, the amplitude becomes zero. First graph shows the voltage difference between the two subcircuit A. Synchronizations and un-synchronized burst appear alternately in a random way. The second graph shows the voltage difference between subcircuit A and subcircuit B. These are not synchronized at all. The third and fourth graphs show the voltage differences between two subcircuit B. In the Systems 1 and 3, similar results are observed.

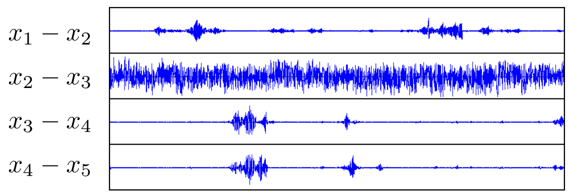

Fig. 7. Voltage differences between two subcircuits in the case of System 2.

Next, the relationship between the synchronization and small parameter mismatches are investigated. In order to investigate it, the synchronization is defined as following equation and figure.

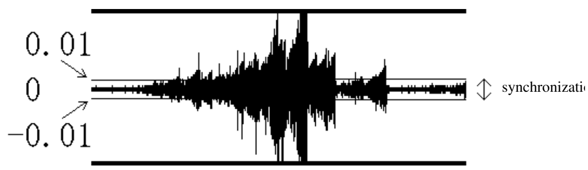

Fig. 8. Definition of the synchronization.

$$|x_k - x_{k+1}| < 0.01 \qquad (10)$$

Figure 9 shows ratios of the synchronization time and total time in the case of System 1. Q is shown as following equation.

$$q_k = Q(k-1) \qquad (11)$$

Q is corresponding to small parameter mismatches q_k of subcircuit B group. By increasing small parameter mismatch

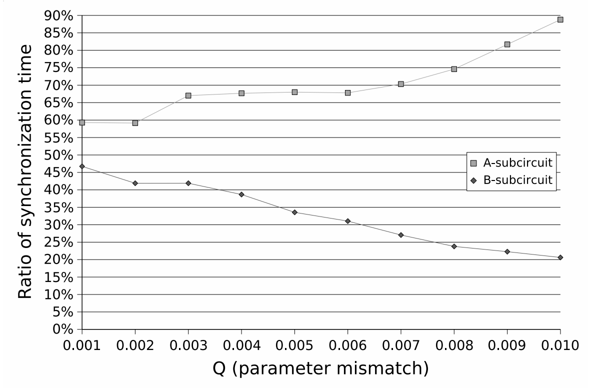

Fig. 9. Relationship of the ratio of the synchronization time and small parameter mismatches in the case of System 1. $m = 2$, $n = 3$, $p_k = 0.001(k-1)$, $\alpha = 0.400$, $\beta = 0.500$, $\gamma = 20.0$ and $\delta = 0.070$

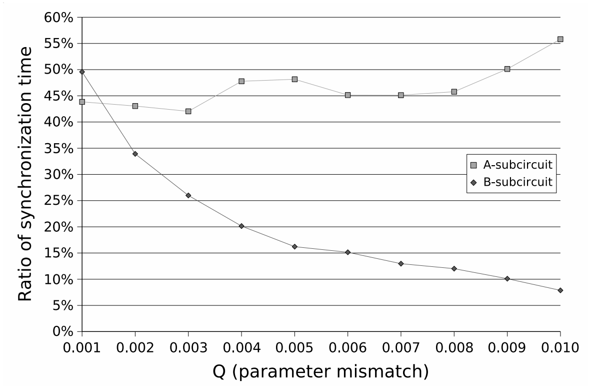

Fig. 10. Relationship of the ratio of the synchronization time and small parameter mismatches in the case of System 2. $m = 2$, $n = 3$, $p_k = 0.001(k-1)$, $\alpha = 0.600$, $\beta = 0.500$, $\gamma = 20.0$, $\delta = 0.070$, $\varepsilon = 0.6$, $\zeta = 1.5$ and $\eta = 0.5$.

of subcircuit B group, the synchronization time of subcircuit A group is increased. Namely, in spite of increasing small parameter mismatches of the system, the synchronization time of subcircuit A group is increased. Figure 10 and Figure 11 show the case of System 2 and 3, respectively. In these case, periodic orbits are observed on some value Q. In particular, $Q = 0.004$ and $Q = 0.005$ in the case of System 2 and $Q = 0.08$ in the case of System 3. Excepting periodic orbits, the synchronization time of subcircuit A group is also increased by increasing small parameter mismatch of subcircuit B group. On all systems, we can also observe the case of decreasing the synchronization time when increasing small parameter mismatches of subcircuit B group in other parameters of subcircuit A group and B group. We suppose that the phenomenon can be explained as follows. The synchronizations of the one subcircuit group and the other subcircuit group are constricted each other. Therefore, in the case of decreasing the synchronization of one group, the synchronization of the other group increases.

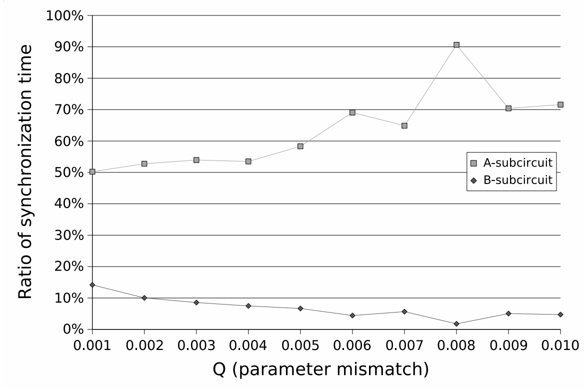

Fig. 11. Relationship of the ratio of the synchronization time and small parameter mismatches in the case of System 3. $m = 2$, $n = 3$, $p_k = 0.001(k-1)$, $\alpha = 0.600$, $\beta = 0.400$, $\gamma = 100.0$, $\delta = 0.060$, $\varepsilon = 1.4$, $\zeta = 7$, $\eta = 0.5$, and $\theta = 1.2$.

IV. CONCLUSION

In this study, three kinds of asymmetrical global chaotic coupled systems are proposed and investigated. In the case of five subcircuits, we confirmed synchronization phenomena. Additionally, It was confirmed that the synchronization time ratio of one subcircuit group are increased by decreasing the synchronization time ratio of the other subcircuit group. We suppose that the phenomenon can be explained as follows. The synchronizations of the one subcircuit group and the other subcircuit group are constricted each other. Therefore, in the case of decreasing the synchronization of one group, the synchronization of the other group increases.

REFERENCES

[1] L. M. Pecora and T. L. Carrol, "Synchronization in Chaotic Systems," *Physical Review Letters*, vol. 64, pp. 821–824, 1990.
[2] K. Kaneko, "Clustering, Coding, Switching, Hierarchical Ordering, and Control in a Network of Chaotic Elements," *Physica D*, vol. 41, pp. 137–172, 1990.
[3] H. Sekiya, S. Moro, S. Mori, and I. Sasase, "Synchronization Phenomena on Four Simple Chaotic Oscillators Full-Coupled by Capacitors," *IEICE Trans. fundamentals*, vol. J82-A, No. 3, pp.375–385, 1999.
[4] M. Miyamura, Y. Nishio and A. Ushida, "Clustering in Globally Coupled System of Chaotic Circuits," *IEEE Proc. ISCAS'02*, vol. 3, pp. 57–60, 2002.
[5] Y. Hosokawa, R. Tsujioka and Y. Nishio, "Relation between Synchronous Rate and Small Variations on an Asymmetrical Coupled Chaotic System," *Proc. NOLTA'05*, pp. 166–169, 2005.
[6] M. Shinriki, M. Yamamoto and S. Mori, "Multimode Oscillations in a Modified van der Pol Oscillator Containing a Positive Nonlinear Conductance," *Proc. IEEE*, vol. 69, pp. 394–395, 1981.
[7] N. Inaba, T. Saito and S. Mori, "Chaotic Phenomena in a Circuit with a Negative Resistance and an Ideal Switch of Diodes," *IEICE Trans. fundamentals*, vol. E-70, no. 8, pp. 744–754, 1987.